

The effects of size, shape, and surface composition on the diffusive behaviors of nanoparticles at/across water–oil interfaces via molecular dynamics simulations

Wei Gao · Yang Jiao · Lenore L. Dai

Received: 23 September 2015 / Accepted: 12 March 2016 / Published online: 30 March 2016
© Springer Science+Business Media Dordrecht 2016

Abstract We have employed molecular dynamics simulations to systematically investigate the effects of nanoparticles' structural and chemical properties on their diffusive behaviors at/across the water–benzene interface. Four different nanoparticles were studied: modified hydrocarbon nanoparticles with a mean diameter of 1.2 nm (1.2HCs), modified hydrocarbon nanoparticles with a mean diameter of 0.6 nm (0.6HCs), single-walled carbon nanotubes (SWCNTs), and buckyballs. We found that the diffusion coefficients of 0.6 and 1.2HCP were larger than the corresponding values predicted using the Stokes–Einstein (SE) equation and attributed this deviation to the small particle size and the anisotropy of the interface system. In addition, the observed directional diffusive behaviors for various particles were well-correlated with the derivative of the potential of mean force (PMF), which might indicate an effective driving force for the particles along the direction perpendicular to the interface. We also found that nanoparticles with isotropic shape and uniform surface, e.g., buckyballs, tend to have smaller diffusion coefficients than those of nanoparticles with comparable dimensions but anisotropic shapes and non-uniform surface composition, e.g., SWCNT and 0.6HCP. One possible hypothesis for this behavior is that the “perfect” isotropic shape and uniform surface of buckyballs result

in a better-defined “solvation shell” (i.e., a shell of solution molecules), which leads to a larger “effective radius” of the particle, and thus, a reduced diffusion coefficient.

Keywords Molecular dynamics simulations · Oil/water interfaces · Buckyball · Carbon nanotube · Surface morphology · Diffusion behaviors

Introduction

The diffusion and self-assembly of nanoparticles at/across liquid–liquid interfaces are important in both natural and industrial applications. For example, the small size of the nanoparticles results in weak confinement of the nanoparticles at the liquid–liquid interface, which opens avenues to size-selective particle assembly (Lin et al. 2003). Furthermore, there is a growing interest in solid-stabilized emulsions (Pickering emulsions) that use solid nanoparticles or microparticles as emulsion stabilizers: small particles can form a layer between the interface of the droplet (dispersed phase) and the continuous phase to inhibit the coalescence of droplets and generate kinetically stable emulsions (Tarimala and Dai 2004). However, the fundamentals of the diffusion and self-assembly of nanoparticles at/across liquid–liquid interfaces have not been fully explored. One of the remaining challenges is to understand multiphase interactions,

W. Gao · Y. Jiao · L. L. Dai (✉)
School of Engineering of Matter, Transport, and Energy,
Arizona State University, Tempe, AZ 85287, USA
e-mail: Lenore.Dai@asu.edu

self-assembly processes, and self-assembled structures of nanoparticles, especially when the size of the nanoparticles is comparable with the molecular dimension of the surrounding liquids (Frost and Dai 2012). For example, there are few reports on the effect of anisotropic particle shapes in Pickering emulsions (de Folter et al. 2014; Ma and Dai 2007). In addition, the kinetics of particle adsorption onto liquid interfaces is also not completely understood (Ma and Dai 2007).

Molecular dynamics (MD) simulations have been a powerful tool for understanding the properties of assemblies of molecules in terms of their structure and the microscopic interactions between them. It serves as a bridge between microscopic length and time scales and the macroscopic world of the laboratory. Besides, MD simulations offer a unique opportunity to explore the microscopic world which cannot be studied by conventional experiments: the hidden details behind bulk measurement can be revealed by MD simulation. For example, Moreira and Skaf (Moreira and Skaf 2004) reported a significant reduction of hydrogen bonds near the water/carbon tetrachloride interface and the dipole moments of water show preference of aligning along the interface. The work by Zhang et al. (Zhang et al. 1995) suggest that there are inner and outer layers near the water–octane interface and that the water dipoles point in opposite directions at the different layers. Recently, Dai's research group has simulated the self-assembly and diffusion of nanoparticles in water–oil, ionic liquid–water, and ionic liquid–oil systems, (Frost and Dai 2012; Song et al. 2010; Luo et al. 2006; Frost et al. 2012; Frost and Dai 2011) providing insights into the transport and interfacial behavior of nanoparticles in liquid–liquid systems. However, systematic numerical investigation of the effects of structural and chemical parameters of nanoparticles on diffusion kinetics at/ across liquid–liquid interfaces has not been carried out and is thus the focus of this work. It is expected that a fundamental understanding of nanoparticle diffusion in liquid systems could be obtained from this study, and a microscopic mechanism theory could be proposed to explain macroscopic observations. In this study, we have demonstrated that MD simulations can provide insight into nanoparticle diffusion in a water–benzene model system. Furthermore, a detailed discussion including simulation system validation, and the effects of size, shape, and surface composition on

the self-assembly and diffusion behaviors of nanoparticles at/ across water–benzene interface is given.

Methodology

All MD simulations were performed using the GROMACS 4.5.4 package (Berendsen et al. 1995). The initial simulation box for each interfacial system was approximately $5.0 \times 5.0 \times 10.0$ nm (Frost and Dai 2011). After the initial configurations were obtained, 1000 energy minimization steps were performed using the steepest descent method. The leapfrog algorithm was used for integrating Newton's equation of motion with a time step of 0.002 ps. We performed NVT [(constant number of molecules, constant volume, and constant temperature)] simulations for calculating the surface tension of benzene/air and benzene/water interfaces, and the Berendsen thermostat (Berendsen et al. 1984) was applied to maintain the system's temperature at 300 K. For simulating the water/oil/nanoparticle system, the NPT [(constant number of molecules, constant pressure, and constant temperature)] ensemble was applied, with the Berendsen thermostat and Berendsen barostat (Berendsen et al. 1984) used to couple the system to a temperature and pressure bath at 300 K and 1 bar, respectively. Periodic boundary conditions (PBC) were applied to all three directions of the simulated boxes. The initial atomic velocities were generated with a Maxwellian distribution at the given absolute temperature. The particle-mesh ewald (PME) method was used for the long-range electrostatic interactions. The cut-off distance for Lennard–Jones forces was set as $r = 1.4$ nm. After the simulation, the physical properties were characterized using the GROMACS analysis tools, and the structures were visualized by visual molecular dynamics (VMD) (Humphrey et al. 1996).

Water was described with a single point charge (SPC) model, which has been proven to perform well in simulating the water–oil system (Luo et al. 2006). The topology and structure of benzene were generated by automated topology builder (ATB) and Repository version 2.1 (Malde et al. 2011). Benzene was described by the Gromos 53A6 force field (Fu and Tian 2011; Oostenbrink et al. 2004; van der Spoel et al. 2012; Schmid et al. 2011), which was validated by the previous researchers (Fu and Tian 2011) as a

reasonable estimation of the real liquid benzene. The geometrical structures of single-walled carbon nanotube (SWCNT) and buckyball were created by Nanotube Modeler. The Gromos 54A7 force field (Schmid et al. 2011) was used to describe SWCNT (Garate et al. 2014; Larin et al. 2015) and buckyball (Lai and Oostenbrink 2012). We also performed simulation with Gromos 53A6 (Oostenbrink et al. 2004) and observed no changes in the system behaviors (Wong-Ekkabut and Karttunen 2012). The spherically modified hydrocarbon nanoparticles (0.6, 1.2HCP) were formed by truncating a diamond-like lattice made of carbon atoms bonded in a non-planar hexagonal structure, and to increase the simulation efficiency, saturated with united CH, CH₂, and CH₃ atoms (Luo et al. 2006; Mazyar and Hase 2006). The force field parameters for 0.6HCP and 1.2HCP were taken from the Gromos 54A7 parameter set (Oostenbrink et al. 2004; Schmid et al. 2011) to simulate rigid hydrophobic particles (Song et al. 2010; Luo et al. 2006). This structure has been used in previous simulation studies focused on interfacial self-assembly (Frost and Dai 2012; Song et al. 2010; Luo et al. 2006a, b; Frost and Dai 2011).

The Potential of Mean Force (PMF) provides information on how the system's energy changes as a function of general "reaction coordinates" (Chandler 1978; Kirkwood 1935). In this report, PMF calculations were used to examine how the system's energy changed as a function of the nanoparticle being pulled from the center of the water phase to the center of the benzene phase with respect to the *z* direction. We took snap shots of this pulling process with the nanoparticle at every 0.15 nm in the *z* direction, for about 5 nm total. These snapshots were then equilibrated for 5 ns each while restraining the particle in its respective position. The force required to restrict the nanoparticle was calculated and analyzed via the weighted histogram analysis method (WHAM) (Roux 1995; Hub et al. 2010; Kumar et al. 1992) and the profile of the PMF of the system in the *z* direction was generated.

Results and discussion

As presented in Fig. 1, the influence of the size of the nanoparticles was investigated by studying two nanospheres with the same surface features (saturated

hydrocarbons) but different sizes, including two types of spherically modified hydrocarbon nanoparticles: 0.6 nm in diameter (0.6HCP) and 1.2 nm in diameter (1.2HCP). The shape effects on the liquid–liquid interface behavior of the nanoparticles were explored by comparing the buckyball and SWCNT, which had the same surface feature (graphene) and comparable size (as indicated in Table 1), but the shape of buckyball was symmetrical whereas the shape of the SWCNT was directional. Detailed information for the nanoparticles is shown in Table 1. Finally, the effects of the nanoparticle's surface composition were investigated by comparing the buckyball and 0.6HCP. Both nanoparticles have the same size and shape. However, the surface of the buckyball consisted of sp² carbon atoms, while the surface of 0.6HCP was composed of saturated hydrocarbons.

Validation of the simulation system

The liquid–liquid interfaces were simulated by placing a cubic water simulation box adjacent to a cubic benzene simulation box. The Gromacs 4.5.4 package contains a pre-equilibrated coordinate file for SPC water, and the water simulation box was verified by previous researchers; (Frost and Dai 2011, 2012; Luo et al. 2006, 2009) so it was unnecessary to again equilibrate and validate the water simulation box.

The benzene boxes were equilibrated under NPT conditions (constant number of molecules, constant pressure, and constant temperature) for 5 ns. The purpose of this step was to make sure that the benzene box had correct density at 1 bar and 300 K. Our simulation indicated that the benzene box achieved equilibrium after 3.7 ns, and the equilibrium density of the benzene box was 859.95 kg/m³. Compared with the experimental value, 873.8 kg/m³ in the literature (Goodwin RD 1988), the error is within 2 %, which suggests that our simulation system can provide reasonably accurate predictions of reality.

The simulation system was also examined by calculating the surface tension of the benzene/air and benzene/water interface. We calculated the surface tensions of benzene/air by doubling the *z* vector of the equilibrated boxes to form a liquid/gas surface, and then performed a 10 ns NVT MD simulation. The simulated value of surface tension of benzene/air was 27.0 ± 2.1 mN/m, which is comparable to the

Fig. 1 Schematic of the SWCNT, buckyball, and hydrocarbon particles used to investigate the effect of shape, size, and surface composition on the diffusion and self-assembly process of nanoparticles at a liquid–liquid interface

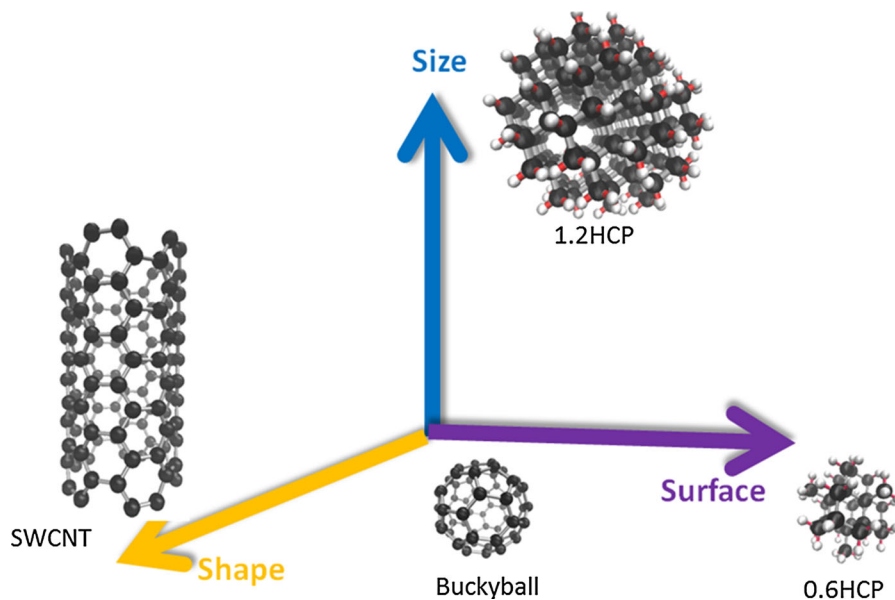


Table 1 Detailed information of the studied nanoparticles

Nanoparticle	Dimension		Carbon number	Hydrogen number
	Radius (nm)	Length (nm)		
SWCNT	0.32	1.2	120	0
Buckyball	0.34	–	60	0
0.6HCP	0.33	–	30	40
1.2HCP	0.62	–	171	128

experimental value of 28.22 mN/m, (Goodwin 1988) indicating a reasonable value of surface tension. To calculate the interfacial tension of benzene/water, we put an equilibrated benzene box adjacent to an equilibrated water box, and then performed a 10 ns NVT simulation. The simulation result of the benzene/water interfacial tension was 35.2 ± 2.7 mN/m. The surface tension measured by Cupple et al. (Cupples 1947) was 32.67 ± 0.05 mN/m, which further indicated that our simulation systems were a reasonable approximation to the real system and its interfacial behavior.

Effect of nanoparticle size

We investigated the effect of size by comparing the 0.6 and 1.2HCP. The diffusion coefficients of nanoparticles are estimated by monitoring the mean square displacement (MSD) as a function of time, using the Einstein relation (Einstein 1905), $\lim_{n \rightarrow \infty} |r_i(t) - r_i(0)|^2 = 6D_A t$,

where $r_i(t)$ is the center of the mass position of the nanoparticle i at time t . The diffusion coefficients of the nanoparticles are calculated by taking the linear regression of the MSD as a function of time. The comparison of the nanoparticles' MSD plots at z direction in water box are indicated in Fig. 2, the inset table lists all the diffusion coefficient calculated from their MSD plots.

The most common basis for estimating diffusion coefficients of particles in liquids is the Stokes–Einstein (SE) equation, (Einstein 1905) $D = \frac{k_B T}{6\pi\eta a}$, where D is the diffusion coefficient, k_B is the Boltzmann's constant, T is the absolute temperature, η is the viscosity of the fluid, and a is the particle radius. In our simulation system, the viscosity of SPC water is 0.30 ± 0.05 cP and we used the simulated viscosities of water to estimate the diffusion coefficients since the nanoparticles are immersed in such media (Song et al. 2010). Table 2 shows that the simulated diffusion coefficients in z direction were

Fig. 2 Mean square displacement (MSD) plots of nanoparticles at z direction in water phase within the first 1 ns. The 0.6HCP is indicated by a solid blue line, 1.2HCP by a dotted red line, SWCNT by a solid purple line and buckyball by a dashed green line. The inset table indicated the diffusion coefficient calculated from the slope of the mean square displacement plots. (Color figure online)

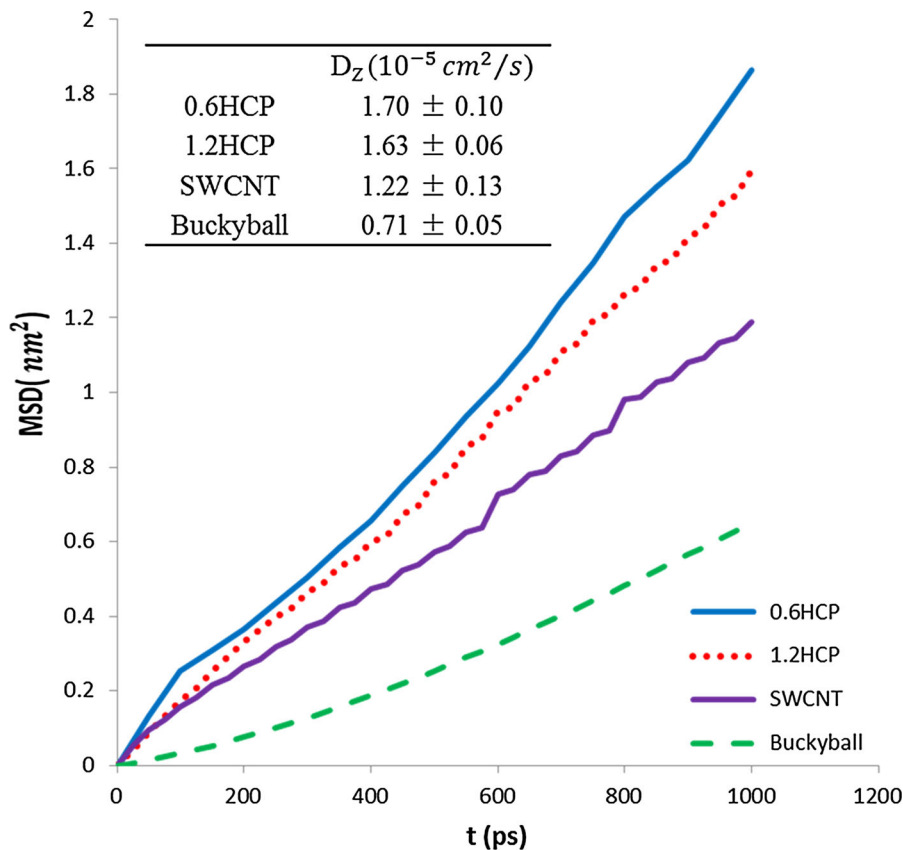


Table 2 Comparison of the nanoparticle diffusion coefficients in the water phase for the MD simulation and the SE equation, respectively

	$D_{MD} (10^{-5} \text{ cm}^2/\text{s})$	$D_{SE} (10^{-5} \text{ cm}^2/\text{s})$
0.6HCP	3.61 ± 0.08	2.52
1.2HCP	4.33 ± 0.15	1.26

larger than those calculated from the SE equation. Previous studies also showed that the diffusion coefficient of nanoparticles was larger than that predicted by the SE equation. For example, Cadmium Selenide nanoparticles were found to diffuse 200 times faster in a polymeric liquid than predicted by the SE equation due to the small size of the nanoparticles (Tuteja et al. 2007). One possible explanation for the failure of the SE equation is that the SE equation is derived by assuming a rigid solute sphere diffusing in a continuum of solvent. When the solute radius is less than five times that of the solvent, the SE equation usually breaks down (Chen 1982). The effectiveness

of the SE equation may even become worse as the solute size becomes smaller and smaller (Cussler 2009). In our simulation, 1.2HCP is approximately 4 times larger than the water molecule (0.27 nm) and the 0.6HCP is about the same size of the water molecule. In addition, the SE equation assumes that the interaction between the particles and the liquids is isotropic. However, in our system, there is a water/benzene interface, which is not isotropic in all three directions. We may indicate how anisotropic our system is by the profile of the PMF: Fig. 3a shows the calculation of the PMF with respect to the z direction for both 0.6 and 1.2HCP, with the approximate position of the water/benzene interface at $z = 0$ nm. The PMF decreases dramatically as the particle approaches the interface. This suggests that our system is directional, that there is a driving force pointing toward the benzene direction. The first derivatives of the PMF are plotted in Fig. 3b, and two observations can be made from Fig. 3b. First, the absolute value of the first derivative of PMF, $d(\text{PMF})/dz$ is larger for 1.2HCP than for

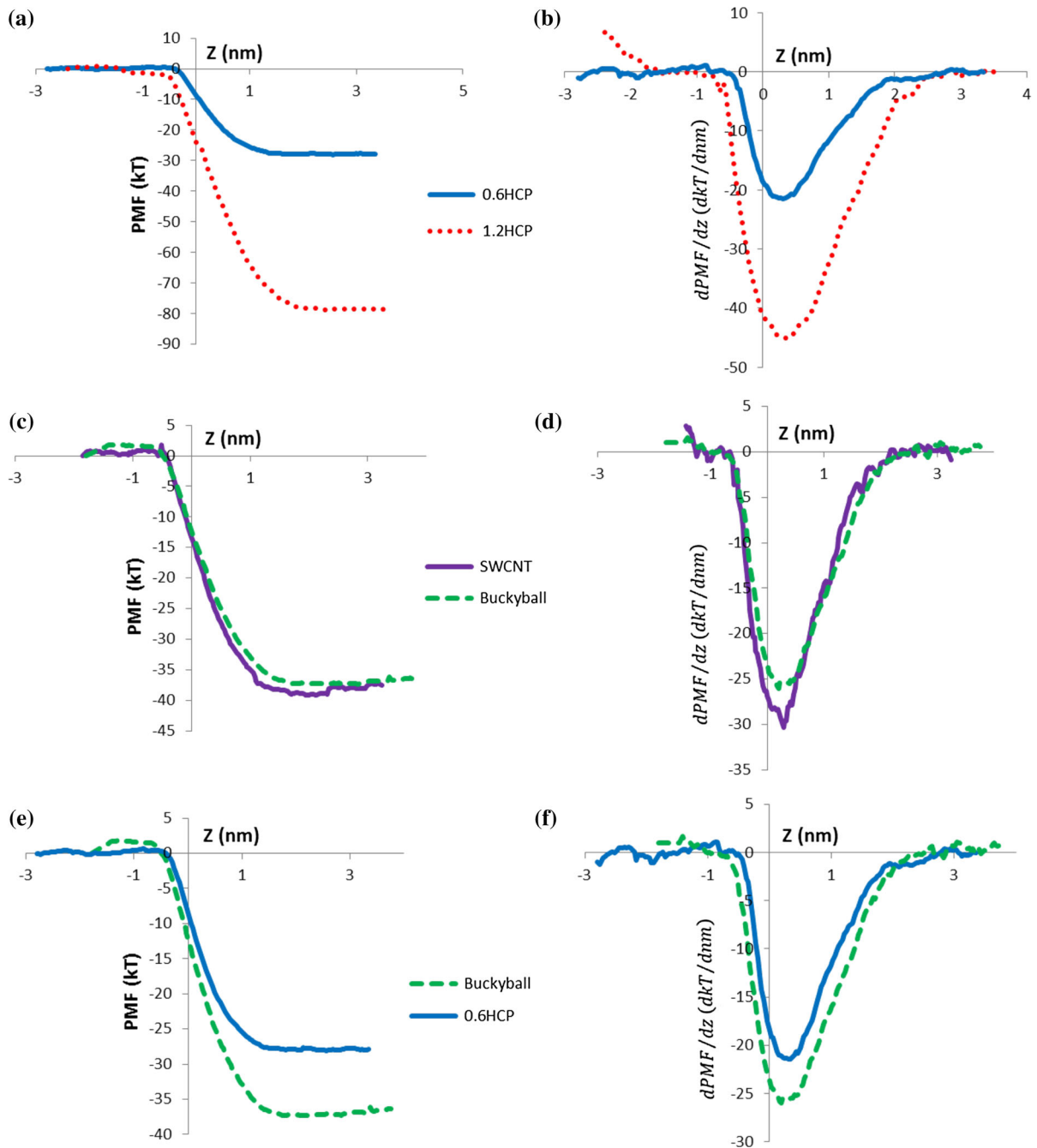


Fig. 3 Plots on the *left* (a, c, e) illustrate comparisons of the potential of mean force (PMF) and plots on the *right* (b, d, f) show the corresponding first derivatives of the PMF for 0.6HCP versus 1.2HCP, buckyball versus SWCNT, and

buckyball versus 0.6HCP. The 0.6HCP is indicated by a *solid blue line*, the 1.2HCP by a *dotted red line*, SWCNT by a *solid purple line*, and the buckyball by a *dashed green line*. The water/benzene interface is at $z = 0$ nm. (Color figure online)

0.6HCP, indicating a stronger driving force on 1.2HCP. According to the estimation of SE equation, the diffusion coefficient of 1.2HCP should be half of 0.6

HCP. However, this study demonstrates that the diffusion coefficients of 1.2 and 0.6HCP are very close to each other, as shown in Fig. 2. Second, the minimum

value of the PMF appears near the interface of benzene/water at the benzene side, which is similar to the calculations of Frost et al. for the hexane/ionic liquid and water/ionic liquid systems (Frost et al. 2012). In the referenced simulations, the minimum value of the PMF also approached the liquid/liquid interface and the nanoparticles eventually equilibrated at positions which correspond to the minimum value of the PMF.

Another interesting observation is that when the nanoparticles pass through the interface, the speed of the large nanoparticles seems to decrease, lingering around the interface at the benzene side for a while. However, the small nanoparticle seems to pass through the interface quite smoothly. Figure 4 shows snapshots of the 0.6 and 1.2HCP at various times, indicating the time necessary for the 0.6 and 1.2HCP to pass through the interface and to the center of the benzene phase. The 1.2HCP “vibrated” and moved laterally near the interface, and it took 4800 ps to move from the interface to the center of the benzene

phase. While for the small particle, it moved to the center of the benzene phase in a quite straightforward manner and it only took 1000 ps. This phenomena maybe explained by the particles’ desorption energy (Bernard and Binks 2006):

$$\Delta G = \pi a^2 \gamma_{ow} (1 \pm \cos\theta)^2,$$

where a is the particle radius, γ_{ow} is the oil–water interfacial tension, and θ is the three-phase contact angle measured through the water phase. The sign inside the bracket is positive for absorption into or desorption from oil and negative for absorption into or desorption from water. This calculation for particle desorption energy quantifies how strongly particles are held at the interface. According to a previous study, (Ma and Dai 2007) for particles with intermediate hydrophobicity in the size range from several nanometers to several microns, the desorption energy is significantly higher than the thermal energy of 1 kT, so the particles are attached at the interface

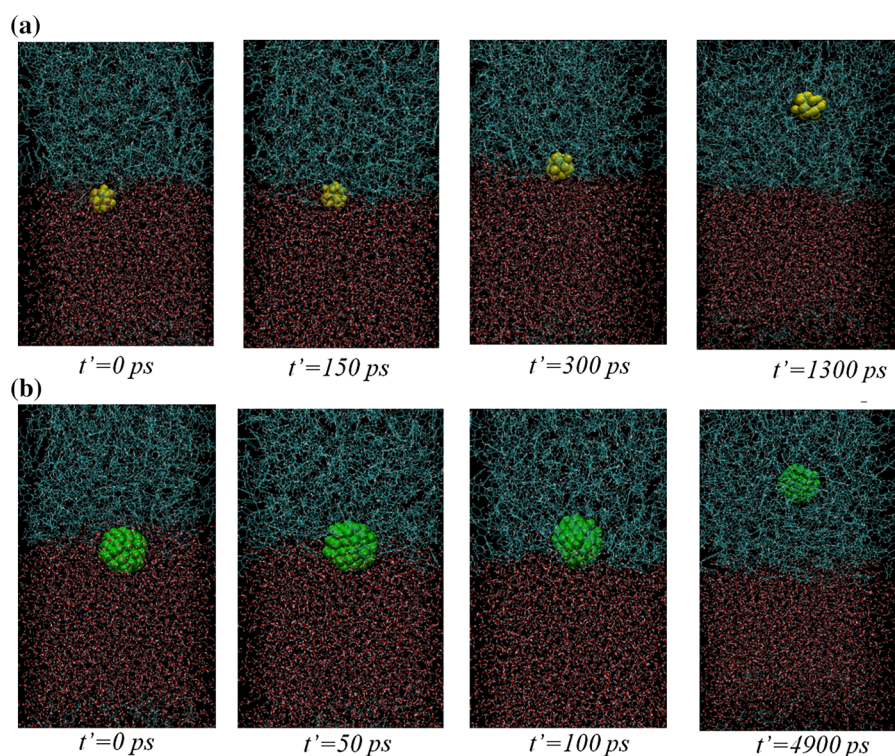


Fig. 4 Snap shots of the nanoparticles at various times. The time was rescaled to compare the time for the movement of the **a** 1.2HCP and **b** 0.6HCP to travel from the water/benzene interface to the approximate center of the benzene phase. The

1.2 and 0.6HCP were represented by *green* and *yellow* ball, and the water and benzene molecules were represented by the *red* and *blue* molecules, respectively. (Color figure online)

irreversibly (Binks 2002). For extremely small particles (radius ≤ 1 nm), the desorption energy becomes comparable to the thermal energy (kT) and the particles might detach from the interface (Binks and Lumsdon 2000). In our simulation, the radius of 1.2HCP is 0.6 nm, thus the effect of the desorption energy is about 9.7 kT , (Ma and Dai 2007) which starts to show its influence, while for the 0.6HCP, the desorption energy is only about 2.4 kT , (Ma and Dai 2007) which is comparable to the thermal energy, so no “hesitation” is observed when the 0.6HCP passes through the interface.

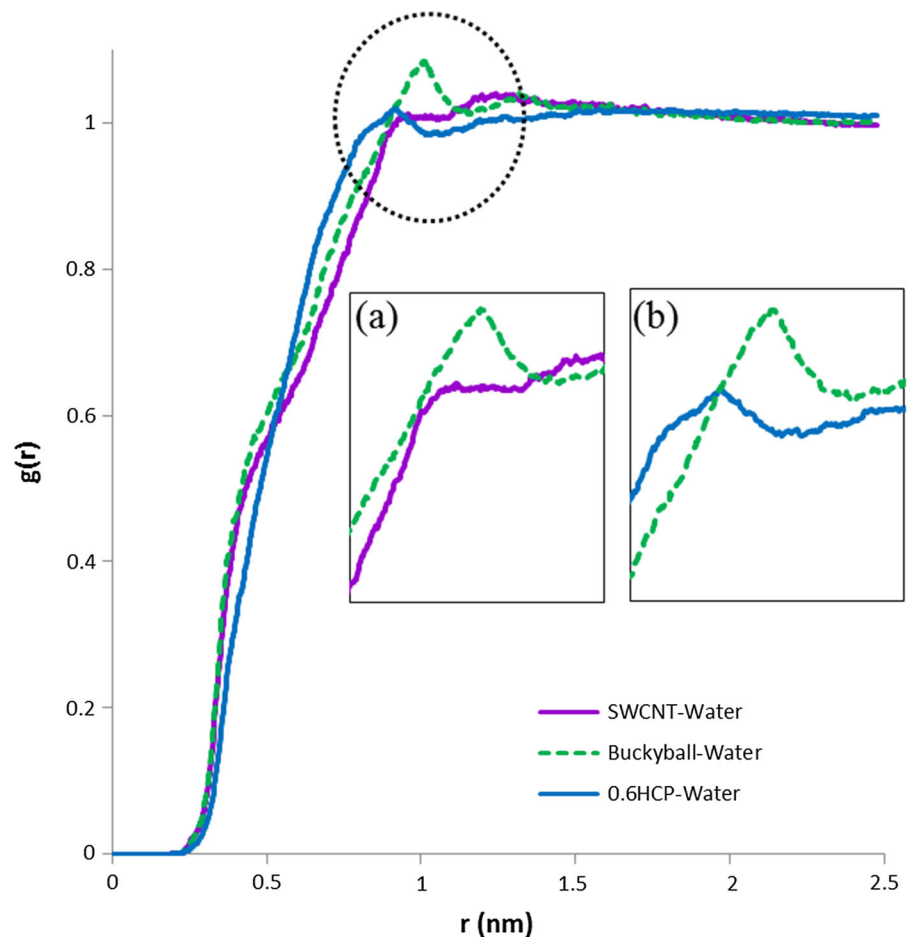
Effect of nanoparticle shape configuration

The effect of a nanoparticle’s shape configuration was investigated by comparing buckyball and SWCNT. Both of them have comparable dimensions (as indicated in Table 1) and the same surface composition

(graphene), but the shape of a buckyball is totally symmetrical, while the shape of a SWCNT is directional. If we compare the MSD of the buckyball and SWCNT in Fig. 2, it is obvious that the diffusion coefficient of SWCNT in the z direction is much larger than that of the buckyball. We calculated the PMF and the numerical differentiation of the PMF for both SWCNT and buckyball. As illustrated in Fig. 3c, d, we can see that the absolute value of the $dPMF/dz$ of the SWCNT is quite close to that of the buckyball. Therefore, we cannot explain the bigger diffusion coefficient of SWCNT by the difference of the driving force on them.

However, if we compare the radial distribution (rdf) functions of the water molecules with respect to the center of mass of the buckyball and SWCNT in the water phase, we can see that there is a notable difference between the buckyball and SWCNT in the rdf plot: as indicated in Fig. 5 [a zoomed-in view of the

Fig. 5 Radial distribution function (rdf) of: water molecules around the buckyball in the water phase, water molecules around the SWCNT in the water phase and water molecules around 0.6HCP in the water phase. Insets **a** and **b** are zoomed-in comparisons of buckyball versus SWCNT and buckyball versus 0.6HCP. The SWCNT is indicated by the *solid purple line*, buckyball by the *dashed green line*, and 0.6HCP by the *solid blue line*. (Color figure online)



comparison between buckyball and SWCNT is illustrated in inset (a)] there is a sharp peak in the rdf plot of the buckyball in water, which indicates an accumulation of solvent molecules surrounding the surface of the buckyball, and also suggests a better-defined solvent layer for the buckyball. The solvent layers around water-solvated species (solvation shell, or hydration shells) have been studied both theoretically and experimentally (Chandler 2005) with particular focus on solvated proteins (Russo et al. 2004; Zhang et al. 2007). A few studies have reported the solvation shells around colloidal particles in both water (Andrievsky et al. 2002) and oil (Storm and Sheu 1995) and suggested that the shells originate from weak interactions between the particle surface and the solvent molecules. We hypothesize that the formation of better-defined solvent layers for the buckyball is due to its shape and the carbon distribution on its surface. Because of the perfect spherical shape of the buckyball, solvent molecules can be packed closely as a spherical shell surrounding its surface. Additionally, because carbon atoms are evenly distributed on the surface of the buckyball, the interaction force between the buckyball and solvent molecules can also form a perfect spherical shell, while for the carbon nanotube there are two open ends, and this uneven distribution of carbon could deform the interaction force field between the carbon nanotube and the solvent molecules and destroy the structure of the “solvent shell” as well. Therefore, the smaller diffusion coefficient of the buckyball may be explained by the formation of the solvent shell: when the buckyball migrates in the solvent, a thickened layer of solvent travels with it. Thus, its “effective radius” (e.g., the radius associated with the “solvent shell”) is actually larger than the radius of the particle itself.

Effect of nanoparticle surface composition

The effect of the surface composition was studied by comparing the buckyball and 0.6HCP, which have a similar shape (spheres) and similar diameters ($d \approx 0.6$ nm), but the surface of the buckyball is made of graphene, while the surface of 0.6HCP is composed of saturated hydrocarbons. As indicated in Fig. 2, although the 0.6HCP and buckyball have a similar shape and size, the diffusion coefficient of the 0.6HCP is significantly larger than that of the buckyball in water. The PMF of the 0.6HCP and buckyball

is depicted in Fig. 3e, with the numerical differentiation of the PMF illustrated in Fig. 3f. As we can see, the absolute value of the PMF of the 0.6HCP and buckyball is quite close when they are in the water phase. The most noticeable difference between the 0.6HCP and buckyball system is again in their radial distribution function. As illustrated in Fig. 5 [the detailed comparison between buckyball and 0.6HCP is illustrated in inset (b)], the peaks of the radial distribution of water molecules for 0.6HCP are weaker than those of the buckyball. Unlike the surface of the buckyball, the atoms on the surface of the 0.6HCP are not all the same and evenly distributed, which results in the asymmetry of the interaction force field, and thus perturb and distort the structure of the solvation shell. Although the buckyball and 0.6HCP have the similar sizes, the solvent layers make the effective radius of the buckyball larger than that of the 0.6HCP causing a smaller diffusion coefficient of the buckyball compared to the 0.6HCP.

Conclusion

In this paper, we have systematically investigated the effects of size, shape, and surface composition on the diffusive behaviors of nanoparticles at/across water–oil interfaces via molecular dynamics simulations. Specifically, four different types of nanoparticles were studied. We found that the diffusion coefficients of the 0.6 and 1.2HCP are larger than that predicted by the SE equation. We attribute the deviation from the SE equation to two reasons: first, because the particle size is comparable to the size of the solvent molecules, the viscosity in the original SE equation is overestimated, and certain modifications are needed; second, the anisotropy of the system also makes the diffusion coefficients for the nanoparticles different from the estimation of the SE equation. We then proposed that the first derivative of the PMF ($d(\text{PMF})/dz$) serves as a driving force in the z direction. In addition, the simulation indicates that the solvation shell of the nanoparticles is influenced by their shape and surface geometry. A highly symmetrical nanoparticle with uniform surface such as a buckyball may lead to a uniform interaction force field with the solvent molecules, so that a better-defined solvation shell is formed, and this solvation shell makes the “effective radius” of the nanoparticle larger than its own radius,

which causes a decrease in the diffusion coefficient. We will further investigate this hypothesis by conducting simulations of nanoparticles with different shapes and surface chemistries.

Acknowledgments We are grateful for the support and help of the group member Stella Nickerson who trained Wei in the use of Gromacs software. We also would like to acknowledge the contributions of Dr. Swapnil Kohale and Professor William L. Hase from Texas Tech University who assisted in creating the 0.6HCP particle. Finally, we thank the Arizona State University Fulton High Performance Computing Initiative (HPCI) for providing us access to the supercomputer.

References

- Andrievsky GV, Klochov VK, Bordyuh AB, Dovbeshko GI (2002) Comparative analysis of two aqueous-colloidal solutions of C60 fullerene with help of FTIR reflectance and UV–Vis spectroscopy. *Chem Phys Lett* 364:8–17
- Berendsen HJC, Postma JPM, van Gunsteren WF, DiNola A, Haak JR (1984) Molecular dynamics with coupling to an external bath. *J Chem Phys* 81:3684
- Berendsen HJC, Vandespoel D, Vandrunen R (1995) GRO-MACS—a message-passing parallel molecular-dynamics implementation. *Comput Phys Commun* 91:43–56
- Bernard P, Binks TSH (2006) Diffusion: mass transfer in fluid systems. Cambridge University Press, Cambridge
- Binks BP (2002) Particles as surfactants—similarities and differences. *Curr Opin Colloid Interface Sci* 7:21–41
- Binks BP, Lumsdon SO (2000) Influence of particle wettability on the type and stability of surfactant-free emulsions. *Langmuir* 16:8622–8631
- Chandler D (1978) Statistical mechanics of isomerization dynamics in liquids and the transition state approximation. *J Chem Phys* 68:2959
- Chandler D (2005) Interfaces and the driving force of hydrophobic assembly. *Nature* 437:640–647
- Chen S-H (1982) Tracer diffusion in polyatomic liquids. III. *J Chem Phys* 77:2540
- Cupples HL (1947) Interfacial tension by the ring method: the benzene–water interface. *J Phys Colloid Chem* 51:1341–1345
- Cussler EL (2009) Diffusion: mass transfer in fluid systems. Cambridge University Press, Cambridge
- de Folter JWJ, Hutter EM, Castillo SIR, Klop KE, Philipse AP, Kegel WK (2014) Particle shape anisotropy in Pickering emulsions: cubes and peanuts. *Langmuir* 30:955–964
- Einstein A (1905) Über die von der molekularkinetischen Theorie der Wärme geforderte Bewegung von in ruhenden Flüssigkeiten suspendierten Teilchen. *Ann Phys* 322:549–560
- Frost DS, Dai LL (2011a) Molecular dynamics simulations of nanoparticle self-assembly at ionic liquid a water and ionic liquid a oil interfaces. *Langmuir* 27:11339–11346
- Frost DS, Dai LL (2012) Molecular dynamics simulations of charged nanoparticle self-assembly at ionic liquid-water and ionic liquid–oil interfaces. *J Chem Phys* 136:084706
- Frost DS, Machas M, Dai LL (2012) Molecular dynamics studies on the adaptability of an ionic liquid in the extraction of solid nanoparticles. *Langmuir* 28:13924–13932
- Fu C-F, Tian SX (2011) A comparative study for molecular dynamics simulations of liquid benzene. *J Chem Theory Comput* 7:2240–2252
- Garate JA, Perez-Acle T, Oostenbrink C (2014) On the thermodynamics of carbon nanotube single-file water loading: free energy, energy and entropy calculations. *Phys Chem Chem Phys* 16:5119–5128
- Goodwin RD (1988) Benzene thermophysical properties from 279 to 900 K at pressures to 1000 bar. *J Phys Chem Ref Data* 17:1541
- Hub JS, de Groot BL, van der Spoel D (2010) g_wham—a free weighted histogram analysis implementation including robust error and autocorrelation estimates. *J Chem Theory Comput* 6:3713–3720
- Humphrey W, Dalke A, Schulten K (1996) VMD: visual molecular dynamics. *J Mol Graph* 14:33–38
- Kirkwood JG (1935) Statistical mechanics of fluid mixtures. *J Chem Phys* 3:300
- Kumar S, Bouzida D, Swendsen R (1992) The weighted histogram analysis method for free-energy calculations on biomolecule. I. The method. *J Comput Theory* 13:1011–1021
- Lai B, Oostenbrink C (2012) Binding free energy, energy and entropy calculations using simple model systems. *Theor Chem Acc* 131:1–13
- Larin SV, Glova AD, Serebryakov EB, Nazarychev VM, Kenny JM, Lyulin SV (2015) Influence of the carbon nanotube surface modification on the microstructure of thermoplastic binders. *RSC Adv* 5:51621–51630
- Lin Y, Skaff H, Emrick T, Dinsmore AD, Russell TP (2003) Nanoparticle assembly and transport at liquid–liquid interfaces. *Science* 299:226–229
- Luo M, Mazyar OA, Zhu Q, Vaughn MW, Hase WL, Dai LL, March RV, Final I, May F (2006a) Molecular dynamics simulation of nanoparticle self-assembly at a liquid–liquid interface 22:6385–6390
- Luo M, Mazyar OA, Zhu Q (2006b) Molecular dynamics simulation of nanoparticle self-assembly at a liquid–liquid interface. *Langmuir* 22:6385–6390
- Luo M, Song Y, Dai LL (2009) Heterogeneous or competitive self-assembly of surfactants and nanoparticles at liquid–liquid interfaces. *Mol Simul* 35:773–784
- Ma H, Dai LL (2007) Particle-laden emulsions. In: Taylor & Francis Online: particle laden emulsions—encyclopedia of surface and colloid science, Second Edition. Taylor & Francis, pp 1–17
- Malde AK, Zuo L, Breeze M, Stroet M, Poger D, Nair PC, Oostenbrink C, Mark AE (2011) An automated force field topology builder (ATB) and repository: version 1.0. *J Chem Theory Comput* 7:4026–4037
- Mazyar OA, Hase WL (2006) Dynamics and kinetics of heat transfer at the interface of model diamond [111] nanosurfaces. *J Phys Chem A* 110:526–536
- Moreira NH, Skaf MS. (2004) Structural characterization of the H2O/CCl4 liquid interface using molecular dynamics simulations. *Progr Colloid Polym Sci*
- Oostenbrink C, Villa A, Mark AE, van Gunsteren WF (2004) A biomolecular force field based on the free enthalpy of

- hydration and solvation: the GROMOS force-field parameter sets 53A5 and 53A6. *J Comput Chem* 25:1656–1676
- Roux B (1995) The calculation of the potential of mean force using computer simulations. *Comput Phys Commun* 91:275–282
- Russo D, Hura G, Head-Gordon T (2004) Hydration dynamics near a model protein surface. *Biophys J* 86:1852–1862
- Schmid N, Eichenberger AP, Choutko A, Riniker S, Winger M, Mark AE, van Gunsteren WF (2011) Definition and testing of the GROMOS force-field versions 54A7 and 54B7. *Eur Biophys J* 40:843–856
- Song Y, Luo M, Dai LL (2010) Understanding nanoparticle diffusion and exploring interfacial nanorheology using molecular dynamics simulations. *Langmuir* 26:5–9
- Storm D, Sheu E (1995) Characterization of colloidal asphaltic particles in heavy oil. *Fuel* 74:1140–1145
- Tarimala S, Dai LL (2004) Structure of microparticles in solid-stabilized emulsions. *Langmuir* 20:3492–3494
- Tuteja A, Mackay ME, Narayanan S (2007) Breakdown of the continuum Stokes–Einstein relation for nanoparticle diffusion. *Nano Lett* 7:1276–1281
- van der Spoel D, van Maaren PJ, Caleman C (2012) GROMACS molecule & liquid database. *Bioinformatics* 28:752–753
- Wong-Ekkabut J, Karttunen M (2012) Assessment of common simulation protocols for simulations of nanopores, membrane proteins, and channels. *J Chem Theory Comput* 8:2905–2911
- Zhang Y, Feller SE, Brooks BE, Pastor RW (1995) Computer simulation of liquid/liquid interfaces. I. Theory and application to octane/water. *J Chem Phys* 103:10252–10266
- Zhang L, Wang L, Kao Y (2007) Mapping hydration dynamics around a protein surface. *Proc Natl Acad Sci USA* 104:18461–18466